RESEARCH APPROACHES TO THE PROBLEM OF REENTRY COMMUNICATIONS BLACKOUT

By Paul W. Huber and Theo Sims

NASA Langley Research Center
Langley Station, Hampton, Va.

Presented at the Third Symposium on the Plasma Sheath
Sponsored by Air Force Cambridge Research Laboratories

September 21-23, 1965
Boston, Massachusetts

[redacted]

L-4591

RESEARCH APPROACHES TO THE PROBLEM OF

REENTRY COMMUNICATIONS BLACKOUT

By Paul W. Huber and Theo Sims

NASA Langley Research Center
Langley Station, Hampton, Va.

ABSTRACT 29449

In order to significantly reduce the constraints on radio-link systems due to reentry blackout, it is necessary to define accurately the extent of the blackout region and to develop methods for reducing its extent. The achievement of these goals will, however, require considerable improvement in knowledge of chemical-kinetics plasma processes, of boundary layers and separated plasma flows with ablation contamination, and of em-wave propagation from plasma covered antennas.

Research efforts directed toward the improved understanding of fundamental plasma processes and em-wave propagation are described. It is shown that certain aspects of the problem are accessible to simulation in ground facilities and that small-scale flight experiments and piggyback experiments can be useful for supplementing knowledge in those areas not obtainable on the ground. Based on projected research efforts, significant improvement in the required knowledge should be forthcoming. Generalized blunt-body reentry blackout bounds, as based on state-of-the-art knowledge, are presented. It is shown that reentry blackout extent for a given body can be minimized through the choice of signal frequency and antenna location. Factors influencing antenna location include the configuration and type of separated plasma fluid, as well as the nonequilibrium nature of the inviscid and boundary-layer flow.

[redacted]

INTRODUCTION

Almost everyone is familiar with the fact that the reentry communications problem is caused by the high concentration of free electrons which are generated in the flow regions around reentry vehicles.[1] It is also generally understood that, for a large reentry vehicle, a communications blackout typically occurs when the electron concentration in the plasma near an antenna reaches or exceeds a certain critical number which corresponds to the given signal frequency - that is, when $N_e \approx N_{e,cr}$ where $N_{e,cr} \sim f^2$. Based solely on this criterion, therefore, two obvious directions for the reduction or circumvention of the problem are indicated: (1) increase the signal frequency to a point where its critical electron value will clearly be higher than the plasma value, and/or (2) lower the plasma electron concentration by modifying the plasma (for example, by injecting a material which accelerates electron depletion). These two directions are, in fact, the most usable ones within the present state of the art[2,3,4] even though there are other possibilities.

In any case, before mission designers can compute the magnitude of signal loss caused by the plasma, can define the points in the reentry at which the signal will be lost, or can evaluate the magnitude of alleviation required to avoid the signal loss, two parts of the problem must be understood: (1) specification of the plasma electron concentration (based on flow-field knowledge), and (2) determination of the electron concentration which can be tolerated for a given vehicle and antenna (based on electromagnetic-wave-propagation knowledge).[5] Both of these electron concentration levels must be determined quantitatively, since the magnitude of the signal loss [redacted] with the magnitude of their difference.

[redacted]

In this paper, research and state of knowledge regarding the properties of the fluids about blunt reentry bodies are discussed, and the implications of these fluids on the communications problem are indicated. It is also shown that flight experiments can be very useful for study of plasma and em-wave propagation problems in regimes not accessible to ground simulation.

SYMBOLS

C_p pressure coefficient

d_b body diameter, ft

f signal frequency, cps

H fluid enthalpy

k_r recombination rate constant

M any third body

N_e electron concentration, cm^{-3}

$N_{e,cr}$ critical electron concentration, $\frac{f^2}{8.06 \times 10^7}$, cm^{-3}

p_s vehicle stagnation pressure

s distance along streamline

s^* distance along streamline to first point where $N_e = N_{e,eq}$

u fluid velocity, fps

X any neutral species

Δ_{ns} shock-wave standoff distance at nose

ρ fluid density

Subscripts:

a antenna

eq equilibrium

s stagnation point or nose flow

∞ free stream

REENTRY PLASMA CONFIGURATION

Figure 1 is a schematic representation of continuum flow-field regions near typical reentry bodies and illustrates the fact that several distinctly different types of plasma may be present. The outer region (between the shock wave and viscous layers) consists of inviscid air which is first compressed and heated by a strong bow shock wave, at which time free electrons are produced. When this fluid expands around the vehicle, some of the electrons and ions recombine, but, in general, this flow is never in complete chemical equilibrium.

There is a viscous boundary-layer region close to the body surface where fluid is decelerated from the inviscid flow velocity to zero velocity at the surface. There may be additional electron production within the layer, or there may be primarily recombination, depending upon the aerodynamics involved. Due to the ablation of surface material during reentry, this fluid may furthermore be a reacting mixture of air and ablation products. As in the case of the inviscid plasma, the boundary-layer plasma is generally not in equilibrium.

The inner plasma region (between the free-shear layer and the rear-body surfaces) is one of viscous separated fluid which is composed of boundary-layer air "contaminated" with ablation material from the heat shield. This separated mixture recirculates in the base-flow region and is finally scavenged into the wake. Because of the long dwell time of this fluid, the separated plasma is likely to approach equilibrium.

Depending upon the aspect angle, attitude, and roll orientation of the reentry vehicle, signal propagation from an antenna on the body will be through both the inviscid plasma and one of the viscous plasma regions. It will never be through a viscous region only, or the inviscid region only. Since the general problem involves propagation through all these plasmas, it is therefore necessary to determine the electron concentration in each type of plasma.

INVISCID PLASMA PROPERTIES

For determination of the inviscid-flow plasma properties, it is necessary to consider the finite rates at which changes in chemical composition occur with respect to flow rates. Figure 2 is a reentry chemical-kinetics map which helps to illustrate this. The shaded areas represent boundaries of ionic chemical-kinetics regimes for blunt bodies of from 1 foot to 12 feet in diameter, where the upper edge of an area (high-altitude edge) is the boundary for the largest (12-foot-diameter) body.

Only at altitudes above or below those within the reentry map is it permissible to ignore the rates at which ionic reactions occur. For example, at very high altitudes where the fluid density is very low and reaction rates are very slow, there is negligible production of electrons during the flow-dwell time over the vehicle ("negligible" herein means $N_e \lesssim 10^9$ cm^{-3}, which value is the highest tolerable value for VHF transmission frequencies) and therefore the rate values are not important. At altitudes below the lowest boundary, reaction rates are very fast in relation to flow rates because of the high fluid densities and, again, the actual values of the rates may be ignored since complete equilibrium may be assumed.

For large portions of typical reentry trajectories, however, the values of the reaction rates cannot be ignored. In the altitude range between the upper two boundaries shown, the reaction rates, although somewhat slow, are by no means negligible, and both the production processes and recombination processes are nonequilibrium. At altitudes below the next to highest boundary, the electron concentration in the high-density nose region may approach, or be somewhat above, the complete equilibrium value before expanding around the body, although the neutral species may be still short of equilibrium. The expanding body flow is - again - one of nonequilibrium recombination. At altitudes below the next to the lowest shaded area (note the reduced extent along the velocity scale), the ionic chemistry in the aft flow may approach local equilibrium (ions in equilibrium with the local nonequilibrium neutral species)* although the value of the electron concentration is not the complete equilibrium value. Complete equilibrium is achieved only below the lowest altitude boundary where three-body recombinations of the atoms are no longer frozen.

The map is also divided into velocity regimes because the number and types of ionic reactions which can occur in the flow field are a function of the flow enthalpy. In the lowest velocity regime, A, 90 percent or more of the ions produced in the flow field are molecular ions; the ion-production

---

*Since this boundary is a result of faster two-body recombination, it does not extend into the high-velocity, atomic-ion regime. However, if three-body ionic recombination involving electrons as the third body is found to be fast,[6] this bound may extend into the high-velocity regime.

processes are atom-atom and the recombination processes are of the two-body dissociative type. Both processes must be treated using finite rates. The principal ionic reaction is

$$N + O + 2.77 \text{ eV} \rightleftharpoons NO^+ + e^- \tag{1}$$

In the highest velocity regime of the map, C, a completely different situation exists - essentially all the ions produced are atomic ions and recombinations occur only by slow three-body processes, namely

$$O^+ + e^- + M \rightleftharpoons O + M + 13.61 \text{ eV} \tag{2}$$

$$N^+ + e^- + M \rightleftharpoons N + M + 14.54 \text{ eV} \tag{3}$$

where M is any third body. Two-body recombination processes are largely excluded in this regime (even considering charge transfer) since the appropriate molecular species represent less than 10 percent of the ionic species. Because the three-body processes are slow at typical reentry fluid-density levels, it is therefore often correct to assume that very few of the ions produced at the nose of the vehicle recombine in the subsequent expanded body flow (i.e., frozen ionic recombination). Hence, the electron concentrations will be very high in this regime. The production processes are also different in this regime due to the importance of the direct electron impact ionizations at high enthalpy. These ionizations are

$$e^- + X + E \rightleftharpoons X^+ + e^- + e^- \tag{4}$$

where X is any of the neutral species (atomic or molecular) and E is the required energy.

In the middle velocity regime, B, both molecular and atomic ions are present in the plasma, and a class of reactions called charge transfers becomes very important in both the production and recombination aspects of the flow, even though these reactions directly produce no net change in the ionization level. Their importance lies in the fact that the charge transfers are fast relative to other ionic processes and provide an indirect path for the production and depletion of atomic ions, which is more rapid than direct ionization and recombination of atomic species at these velocities. For example, the dominant ionization and recombination processes in this regime are

$$N + O + 2.77 \text{ eV} \rightleftarrows NO^+ + e^- \quad (1)$$

$$N + N + 5.84 \text{ eV} \rightleftarrows N_2^+ + e^- \quad (5)$$

$$O + O + 6.96 \text{ eV} \rightleftarrows O_2^+ + e^- \quad (6)$$

By the transfer of charge from these molecular ions to the atoms O and N, significant "production" of atomic ions can take place within typical nose-flow dwell times. Perhaps even more important is the reverse of this process (charge transfer from atomic ions to molecular species), since a path is provided for the finite-rate depletion of electrons in the expanded flow by means of two-body dissociative recombination. Without this path, the atomic ions might be frozen because of slow three-body recombination. Since the dominant two-body recombination is $NO^+ + e^-$ in this velocity regime, as well as in regime A, the dashed line shown represents the point at which the NO concentration in the equilibrium nose flow equals the atomic-ion concentration. This is another way of saying that a two-body recombination path is available for all the ions produced. The charge transfer path referred to actually consists of a large group of reactions (20 or more), in some only charge is transferred and in others a simultaneous transfer of charge and exchange of atoms occurs.[7]

The real problem in regard to the reentry chemical-kinetics picture is that many of the important reaction-rate constants and their temperature dependencies are not well known. In fact, the currently estimated uncertainties in rates are so large in the medium- and high-velocity regimes that the overall uncertainties in the flow-field electron concentrations amount to factors of from 10 to 30. It is obvious that much improvement in this knowledge is required if plasma computations are to be made with confidence in these regimes.

INVISCID PLASMA SIMULATION

A logical place to study plasma processes is in ground facilities, where attempts can be made to simulate the reentry flow (or at least to isolate some of the significant processes of the reentry flow) and to measure changes in ionic concentration. One of the most useful classes of facilities for this purpose is the shock tunnel and shock tube.

Shock tunnel.- In figure 3, the reentry simulation capabilities of present shock tunnels are shown superimposed on the reentry chemical-kinetics map of figure 2. Two methods in current use are illustrated: complete simulation and stagnation streamline simulation. The upper shaded area represents the complete simulation method in which the reflected shock flow of a shock tube is expanded through a hypersonic nozzle to ambient flight conditions u_∞ and ρ_∞. The high stagnation enthalpy conditions in the shock tube permit such an expansion. A model can be mounted in this flow and measurements can be made. There are, however, several limitations to this method. Because extremely high shock-tube pressures are required, there is a structural limit to the operating range as indicated by the line labeled "high-pressure limit." Furthermore, the expanded nozzle flow does not duplicate the ambient air composition due to nonequilibrium recombination in the nozzle. Because of this nonequilibrium, the clearly valid simulation range is in a lower altitude regime wherein the nose flow can reach equilibrium as in the flight situation. The complete simulation method is useful, however, for studies in the low-velocity reentry regime.[8,9]

Stagnation streamline simulation, as shown by the lower shaded area, is accomplished by expanding the reflected shock-tube flow through a nozzle which is shaped to duplicate the expansion of a vehicle flow-field streamline (to a Mach number of approximately 4) which originates at, or near, the stagnation point. The flight total enthalpy H_s and vehicle stagnation pressure p_s (not free-stream stagnation pressure) must be duplicated in order to permit the simulation. The change in fluid properties along the "streamline" is studied by use of tunnel instrumentation. The primary constraint on this scheme is the large wall boundary layer which develops at the low densities (low Reynolds numbers) required to simulate a flow-field streamline at the higher reentry altitudes. The line in figure 3 labeled "low-pressure limit" indicates the approximate altitude simulation limit due to this constraint. If all the significant reactions were two-body, then the results could be applied also at the higher altitudes by using the binary scaling criterion[10] wherein nonequilibrium effects are duplicated at different altitudes for $\rho_\infty s = \text{Constant}$ at a given flight velocity (s = distance along streamline to a given value of $C_p/C_{p,s}$).

Unfortunately, this is not the case for the low-altitude portions of reentry (high fluid density). In spite of this limitation, however, the method is a very useful one for reentry chemical-kinetics study, since many of the important recombination reactions are thus made accessible. Investigations using this simulation are currently being carried out at the Cornell Aeronautical Laboratory.[6]

Also shown in figure 3 are the reentry paths of small-scale flight-research vehicles used in Project RAM (radio attenuation measurement) at the Langley Research Center of NASA.[5] These are shown to illustrate an experimental approach which provides the capability for plasma and em-wave propagation studies in the reentry areas not accessible to ground simulation.

Shock tube.- The incident shock-wave flow of a shock tube (the flow before reflection or expansion occurs) can be used for study of nonequilibrium production processes. Results of these investigations have application to high-altitude reentry flow in the bow shock region. (Note that normal shocks can be used to simulate the vehicle oblique-shock flow as well.) Since the bow shock region is the principal region for electron production, such studies can yield valuable information about reentry blackout points. Figures 4 and 5 illustrate the nature of the correlation. Note that a finite distance, s^*, is required in the flow behind the shock for the electron concentration to first reach a value which corresponds to the final equilibrium value. (This is not complete equilibrium since the neutral species are generally not in equilibrium dissociation at this point. The overshoot which usually occurs in N_e beyond this point is, in fact, the result of such a condition.) The increase with distance of electron concentration behind the shock is shown in figure 5. For this discussion, the overshoot and the return to complete equilibrium can be ignored. The curve for 23,000-fps flight velocity is based on results given by Lin and Teare,[7] and the curve for high flight velocity ($u > 35{,}000$ fps) is assumed on the basis that electron impact ionization will yield an increase in production rate in the later stages of production.

If (see fig. 4) a typical flow distance in the bow shock region - say Δ_{ns}, the shock standoff distance - is large compared to s^*, the required equilibrium ionization distance, then the flow will certainly come to ionic equilibrium before expanding around the body. However, if the ionization distance becomes very large relative to the standoff distance, as at high altitudes where rates are slow, then the fluid may be far short of ionic equilibrium at the start of the expansion. Since all the production processes are two-body, and the competing three-body recombination processes (for example, neutral atom recombination) can be neglected under conditions short of equilibrium production[10] (again note that at the first point where $N_e = N_{e,eq}$, the fluid is generally short of full equilibrium), it is permissible to use the binary scaling criterion previously mentioned. This criterion was used to establish the boundary for "equilibrium" nose ionization given in figure 2 - that is, the point where $2\Delta_{ns} = s^*$. ($2\Delta_{ns}$ was used as the typical nose flow distance, and $s^* = s^*(u_\infty)$ at an altitude of 250,000 ft was taken from shock-tube results[7] along with extrapolation to higher velocity.)

By making some additional assumptions, the foregoing nonequilibrium shock wave results are used to approximately determine initial reentry blackout points without making complete finite-rate calculations - which are laborious. The first assumption is that, in the flow-expansion region, ionic recombination is frozen at altitudes above the nose equilibrium boundary shown in figure 2. This assumption is valid except for cases in the medium- and low-velocity regimes where the value of N_e is high enough at the start of the expansion to allow significant two-body recombination to occur. The reason for this restriction can be seen from the following relation for two-body electron depletion:

$$\frac{dN_e}{ds} = -\frac{k_r(N_e)^2}{u} \quad (7)$$

where k_r is the reverse rate (for example, eq. (1)) and u is the local fluid velocity. For typical values of k_r and u, the highest allowable N_e for which frozen ionic recombination can be assumed is about 10^{11} cm^{-3}. The second assumption is one of similarity of the frozen ionic expansion, that is, the ratio $N_{e,a}/N_{e,s}$ is invariant with altitude and dependent only on $C_{p,a}/C_{p,s}$, the pressure-coefficient ratio at the antenna. This assumption can be shown to be a reasonably good one.

The following additional steps are then used to complete the determination of a blackout point: (a) At the altitude corresponding to equilibrium N_e at the nose (fig. 2) the electron concentrations at the nose* and at the antenna location are found. (The latter N_e is found by means of a frozen flow expansion from $C_p = C_{p,s}$ to $C_p = C_{p,a}$). (b) As a result of the second assumption above, the ratio $N_{e,a}/N_{e,s}$ has the same value at the equilibrium nose altitude and at the blackout altitude. Since $N_{e,a}$ at the blackout altitude is equal to $N_{e,cr}$ for the signal, it follows that,

---

*The N_e restriction doesn't apply here, since this is merely a fictitious step in the procedure.

$$\frac{N_{e,cr}}{N_{e,a,eq.\ alt.}} = \frac{N_{e,s,B.O.\ alt.}}{N_{e,s,eq.\ alt.}} \tag{8}$$

(c) Using curves such as shown in figure 5, the nose flow distance ratio, s/s^*, is found which corresponds to the electron concentration ratio on the right-hand side of equation (8) above. The distance, s, in this ratio then represents the fraction of the nose flow distance at the equilibrium altitude which grows to the full nose flow distance at the blackout (nonequilibrium production) altitude.

(d) From binary scaling ($\rho_\infty s$ = Constant) of the above nose flow distance ratio, the blackout altitude is then found by determining the altitude at which ambient air density is equal to $\rho_{\infty,B.O.\ alt.}$ in the following equation:

$$\frac{s}{s^*} = \frac{\rho_{\infty,B.O.\ alt.}}{\rho_{\infty,eq.\ alt.}} \tag{9}$$

The application of this method, for example to Mercury-Atlas or Gemini-Titan orbital reentry, yields a VHF blackout altitude of about 313,000 feet, as compared with experimental values of 308,000 to 318,000 feet. The computed blackout altitude is not sensitive to the choice of $2\Delta_{ns}$ as a typical nose flow distance, although the equilibrium nose altitude boundary is sensitive.

Experimental studies of nonequilibrium production chemistry behind shock waves are being carried out by several research groups, including those at Avco-Everett Research Laboratory and Cornell Aeronautical Laboratory. Improved production rate knowledge in the high-velocity regime (electron impact production) is, of course, needed for proper assessment of reentry plasma properties.

BOUNDARY-LAYER PLASMA

As in the case of inviscid plasma, determination of the reentry boundary-layer plasma properties involves consideration of the finite rates at which changes in chemical composition occur. The problem is more complex, however, because the nonequilibrium chemistry includes - in addition to the air species - also the species resulting from reaction of ablation products with the air. Furthermore, the fluid mechanics part of the problem is complicated by the necessity for inclusion of effects due to diffusion, heat conduction and viscosity, which are usually negligible in the inviscid problem. Nevertheless, comprehensive analyses of reentry boundary-layer plasma have been made.[11,12,13,14] In general, the results of studies such as these indicate that this plasma region is of importance in reentry communications primarily for pointed or long slender bodies at low altitudes - say, below 120,000 ft - and for antennas located on the aft parts of the bodies. In such cases, the boundary-layer region is the primary site for electron production and - due to the finite rates involved - this production occurs well back from the nose region (on the order of 10 ft or more). Small amounts of alkali impurities in the ablation material are shown to cause large increases in the boundary-layer electron concentration over that for clean air. On the other hand, the electron concentration in the boundary layer must go considerably higher than $N_{e,cr}$ to cause blackout, since this layer is generally thin in relation to a signal wavelength.

The boundary-layer plasma is less important in blunt body reentry communications for several reasons. First, the inviscid plasma is much thicker for blunt bodies due to the much larger fraction of the flow which passes through the strong bow shock front. Next, due to the lower Mach number in the external flow for blunt-body flow fields, the peak temperature in the boundary layer is not as high relative to the inviscid flow temperature and does not occur as close to the wall.

SEPARATED FLOW PLASMA

Current knowledge regarding separated flow plasma properties is not very refined, although great strides are being made.[15] In order to determine, at least grossly, the possible importance of this plasma region in reentry communications, electromagnetic-wave-propagation results from flights involving separated regions have been studied. For this purpose, results from the Mercury-Atlas reentries have been used, because the separated region completely surrounds the antennas.

Shown in figure 6 are the effective values of flow-field electron concentration as deduced from the propagation results, along with computed values based on several assumed plasma models. The symbols represent the electron concentrations required to produce the observed attenuations when using a plane-wave, slab model of the propagation. (It is interesting that the C-band propagation is such a sensitive diagnostic tool. The electron concentration must be between about 2×10^{11} and 4×10^{11} in order to give attenuation without blackout.) Note, first of all, that the finite-rate inviscid-flow theoretical model (plasma properties along a streamline expanded from the nose region to the antenna region) does not provide a reasonable correlation in the peak N_e part of the reentry, although it appears to be good otherwise. This lack of correlation cannot be attributed to the rate-knowledge uncertainty, so that one must conclude that this plasma was not the significant one for attenuation during the peak N_e

period. A 25 reaction system was used in this model. It is interesting to note that the peak N_e region appears to be flattened; this is a result of increased two-body recombination at the higher values of N_e (see eq. (7)), since there is a sufficiently long dwell time along the streamline (to the rearward antenna location) for this action to be very effective. For this same reason, a rearward antenna location is preferred over a more forward location, and larger bodies - within certain limitations - are preferred over smaller bodies.

The results obtained from a separated plasma model are, however, seen to be much closer to the experimental results. Two principal assumptions are used in this model: (1) the separated fluid is in complete equilibrium, and (2) the effective enthalpy of the fluid is 0.70 of the stagnation fluid enthalpy. By using these assumptions, along with the pressure for the separated flow, the electron concentrations are readily calculated. The first assumption should be a reasonable one since the fluid dwell time in this low-velocity, recirculating region is long; whereas the second assumption is rather arbitrary. It should be noted, however, that the assumed value of $0.70H_s$ for the effective fluid enthalpy is not unreasonable in the light of current knowledge,[16] and the correlation shown in figure 6 is not obtained when using higher or lower assumed values.

In order to obtain good correlation also with the data near the peak heating period of the reentry, the additional assumption is made that ablation impurities are present in the separated fluid during this period. It is assumed that alkali impurities (sodium or potassium) are present in the separated fluid at a peak mole fraction of a little more than 10^{-5} during peak heating. These impurities would be present, of course, due to impurities in the original ablation heat shield before it is vaporized and dissociated. Because the temperature in this fluid region is high, the alkali particles (i.e., the ionizable particles) are assumed to be in atomic form (unreacted). Again, the ablation impurity assumptions are arbitrary but are in line with current knowledge of separated flow ablation contamination.

It can be concluded from the comparisons shown in figure 6 that, although other combinations of assumed enthalpy and impurity level might also correlate the results, there are strong indications that the separated flow plasma is the significant one for attenuation during the peak N_e part of the reentry.

REENTRY BLACKOUT BOUNDS

By application of the plasma concepts previously discussed, estimates of the reentry blackout bounds for large blunt bodies can be made. The additional qualification involved is that the pertinent plasma layer be of sufficient thickness such that blackout occurs at the point, $N_e = N_{e,cr}$. This is believed to be generally the case for blunt bodies of the size, $d_b \gtrsim 1$ ft. Such estimates have been made and are shown in figure 7 for three signal frequencies and two body sizes. For general applicability, the estimates have been made for the body flow condition, $0.01 < C_p/C_{p,s} < 0.02$, which is representative of aft antenna locations on blunt reentry bodies. The separated plasma bounds are shown only where they are higher (higher N_e than the inviscid), but it should be noted that in some cases - for example, the VHF calculations - the bounds for separated and for inviscid plasma are very close (as in fig. 6). For cases where propagation is through both types of plasma (depending on attitude, aspect angle, and roll orientation) the higher of the bounds must, of course, be used.

It is seen, first of all, from the inviscid results shown that the VHF boundaries are the highest of the three frequencies and that the larger body has the higher of the two bounds for this frequency and for the other frequencies in the high-velocity regime. The latter result is due to the larger flow distance available for electron production at the nose along with the nearly frozen recombination in the expansion. It is to be noted next that there is a marked reversal in the body size versus altitude comparison as well as a sharp dip in some of the inviscid bounds at velocities around 26,000 or 27,000 ft/sec. These effects result from the relatively fast two-body ionic recombinations which are dominant in the expanding flow at velocities below these values (refer to the two-body - or N_e limiting - velocity boundary shown in fig. 2). At these lower velocities, the larger bodies have the lower bounds because there is more flow time available in the expansion for this recombination to be effective. It is to be noted, furthermore, that because this recombination has an $(N_e)^2$ dependency (see eq. (7)), the dip is much more pronounced for the X-band bounds because of the higher $N_{e,cr}$ involved. In fact, no dip at all is seen in the VHF bounds because the N_e is too low for the recombination to be significant. The blackout boundary for the smaller body at S-band shows no dip because the flow distance is insufficient for recombination at this value of $N_{e,cr}$. In the case of X-band, the shorter flow length is seen to be nearly as effective as the longer one, due to the strong influence of the N_e limiting effect. These results point up the importance of providing sufficient flow length (by using an aft antenna location, for example) at S-band frequencies to minimize blackout, and of the use of higher signal frequencies, such as X-band, when the flow length cannot be as long.

The separated flow bounds shown have no body size identification since equilibrium flow was assumed for this plasma. It is interesting to note from these results that, at X-band, the separated flow plasma increases blackout for both body sizes in the lower velocity regime, while at S-band, it increases the blackout for the larger body size only. This latter effect is, however, seen to be a very detrimental one. The separated plasma with ablation result is shown only for the S-band frequency since the calculated N_e's for such a plasma are typically below 10^{12} cm^{-3} (that required to influence X-band). There is no significant ablation occurring at the reentry conditions corresponding to the VHF boundaries shown.

Several other remarks can be made regarding the results shown in figure 7. No bounds are shown due to boundary-layer plasma because for large blunt bodies in the continuum flow regime this plasma is not generally a determining one for bounds such as shown, although it must certainly be considered in attenuation estimates. While bounds for pointed or long slender bodies are not presented, boundary-layer plasma knowledge for such bodies does suggest the desirability of forward antenna locations to minimize the attenuation and blackout at low altitudes, which is the reverse of the blunt-body inviscid result. In any case, the results of present reentry plasma knowledge in regards to the communication problem point up the need for employment of other means (such as material addition) to reduce the blackout region for large blunt bodies in the super-orbital reentry regime where blackout is extensive.

In order to improve on estimates such as these, three-dimensional flow-field calculations coupled with improved chemical-kinetics knowledge is necessary for the inviscid flow.[6] Much improvement is also needed in knowledge of the fluid mechanics and chemistry of separated air flows with contamination. Even with the improved plasma knowledge, the electromagnetic-wave-propagation problem must be better understood for antenna configurations in close proximity to plasmas[17] and for propagation involving unsymmetrical plasma configurations.

CONTINUING RESEARCH EFFORT

In order to provide a more reliable basis for the design and planning of reentry communications of spacecraft in the higher velocity earth regimes, as well as for planetary entry, the Langley Research Center (LRC) is continuing its research in these problem areas. The program (Project RAM) has already contributed much to the understanding and reduction of blackout as a result of fundamental research in the areas of plasma processes and electromagnetic-wave propagation.[1,5,17,18,19]

The program involves the use of ground facilities and small-scale flight experiments, supplemented by outside contracts, and the continuing research will have a direct bearing on reentry communications. For example, diagnostic instrumentation (reflectometers[19] and Langmuir probes) on RAM C-B will provide basic plasma data in a regime which cannot be simulated in ground facilities. Furthermore, the most promising method for reduction of blackout for a mission such as Apollo - that of material addition - was conceived and flight demonstrated[3] in the RAM program, and will be further refined in the continuing effort. Demonstration of this scheme for a manned reentry was accomplished in the GT-3 mission.[20] It is interesting to note that, although this experiment involved injection of material into the inviscid flow, the results also suggest the importance of the separated plasma.[16]

Research on wave propagation through plasmas and on the effects of plasmas on antenna performance has resulted in significant advances in knowledge.[1,5,17] The results are, in fact, unique in having provided quantitative propagation data under specifiable flight plasma conditions.

As a result of this program and of work contributed by other research organizations in these categories, it is believed that the reentry communications blackout can be more closely delineated and by the employment of certain physical modifications can indeed be greatly reduced.

CONCLUDING REMARKS

The following points are believed to represent a reasonable assessment of the reentry communications blackout picture as based on current knowledge and projected research:

1. The fluid properties in the inviscid- and viscous-flow regions about the reentry vehicles must be more precisely defined in order to determine quantitatively the extent of or to design means to alleviate the reentry communications blackout.

2. Improved chemical-kinetics knowledge is required to properly define the inviscid plasma.

3. An improved understanding of the separated plasma flow, boundary-layer plasma, and of the effects of ablation impurities in these flows is also required.

4. As a result of continuing research in ground facilities and with small-scale flight experiments it is expected that the more important

refinements needed in inviscid and viscous plasma knowledge, as well as improved understanding of em propagation from plasma-covered antennas, will be forthcoming.

5. In order to minimize blackout effects during reentry, communications frequencies in the X-band range are desirable, and rearward locations of the antennas can also be effective. In some cases, propagation through separated plasmas is detrimental to reentry communications and should be avoided.

6. The reentry communications blackout for large vehicles at superorbital velocity is expected to be extensive and employment of means, such as material addition, to alleviate the signal loss by modification of the plasma may be necessary.

REFERENCES

1. Huber, Paul W.; and Sims, Theo E.: The Entry-Communications Problem. Astronaut. Aeron., vol. 2, no. 10, Oct. 1964, pp. 30-38. (Available also as NASA RP-384.)

2. Brummer, E. A.: X-Band Telemetry Systems for Reentry Research. Paper No. CP 63-663, Inst. Elec. Electron. Engr., Apr. 1963.

3. Cuddihy, William F.; Beckwith, Ivan E.; and Schroeder, Lyle C.: RAM B2 Flight Test of a Method for Reducing Radio Attenuation During Hypersonic Reentry. NASA TM X-902, 1963.

4. Spencer, Dwain F.: An Evaluation of the Communication Blackout Problem for a Blunt Mars-Entry Capsule and a Potential Method for the Elimination of Blackout. Tech. Rept. No. 32-594 (Contract No. NAS 7-100), Jet Propulsion Lab., C.I.T., Apr. 15, 1964.

5. Anon.: Proceedings of the NASA Conference on Communicating Through Plasmas of Atmospheric Entry and Rocket Exhaust. NASA SP-52, 1964.

6. Dunn, M. G.; Daiber, J. W.; and Lordi, J. A.: Nonequilibrium Ionization Phenomena in Apollo Plasma Sheath. (This Symposium.)

7. Lin, Shao-Chi; and Teare, J. Derek: Rate of Ionization Behind Shock Waves in Air. II. Theoretical Interpretations. Phys. Fluids, vol. 6, no. 3, Mar. 1963, pp. 355-375.

8. Eschenroeder, A. Q.; Daiber, J. W.; Golian, T. C.; and Hertzberg, A.: Shock Tunnel Studies of High-Enthalpy Ionized Airflows. Rept. No. AF-1500-A-1 (AFOSR 3025), Cornell Aeron. Lab., Inc., July 1962.

9. Lederman, Samuel; Visich, Marian, Jr.; and Abele, Manlio: Preliminary Results of an Experimental Investigation of the Properties of the Plasma Sheath Around a Hypersonic Reentry Body. PIBAL Rept. No. 856, Polytech. Inst. Brooklyn, Dec. 1964.

10. Gibson, Walter E.: Dissociation Scaling for Nonequilibrium Blunt Nose Flows. ARS J. (Tech. Notes), vol. 32, no. 2, Feb. 1962, pp. 285-287.

11. Pallone, Adrian J.; Moore, Jeffrey A.; and Erdos, John I.: Nonequilibrium, Nonsimilar Solutions of the Laminar Boundary-Layer Equations. AIAA Jour. Vol. 2, No. 10, Oct. 1964.

12. Blottner, F. G.: Nonequilibrium Laminar Boundary-Layer Flow of Ionized Air. AIAA Jour., Vol. 2, No. 11, November 1964.

13. Kane, J. J.: Nonequilibrium Sodium Ionization in Laminar Boundary Layers. AIAA Journal, Vol. 2, No. 9, September 1964.

14. Kane, John J.; and Li, Frank: Ablation Effects on RF Attenuation in the Turbulent Boundary Layer. AIAA Journal, Vol. 3, No. 8, August 1965.

15. Reeves, Barry L.; and Lees, Lester: Theory of the Laminar Near Wake of Blunt Bodies in Hypersonic Flow. Paper No. 65-52, Am. Inst. Aeron. Astronaut., Jan. 1965.

16. Beckwith, Ivan E.; Bushnell, Dennis M.; and Huffman, Jarrett K.: Fluid Mechanics Aspects of the Gemini Reentry Communications Experiment. Paper No. 23. Conference on Langley Research Related to Apollo Mission, NASA SP- . Confidential, June 22-24, 1965.

17. Swift, C. T.; and Hodara, H.: Effects of the Plasma Sheath on Antenna Performance. Presented at 10th Symposium of the AGARD Ionospheric Research Committee on Propagation Factors in Space Communications. Sept. 21-25, 1965, Rome, Italy.

18. Evans, J. S.: Reduction of Free Electron Concentration in a Reentry Plasma by Injection of Liquids. (This Symposium.)

19. Grantham, W. L.: Analysis of Plasma-Sheath Electron Density Measurements at Entry Velocities. (This Symposium - Classified Proceedings.)

20. Schroeder, L. C.: Gemini Reentry Communications Experiment. (This Symposium - Classified Proceedings.)

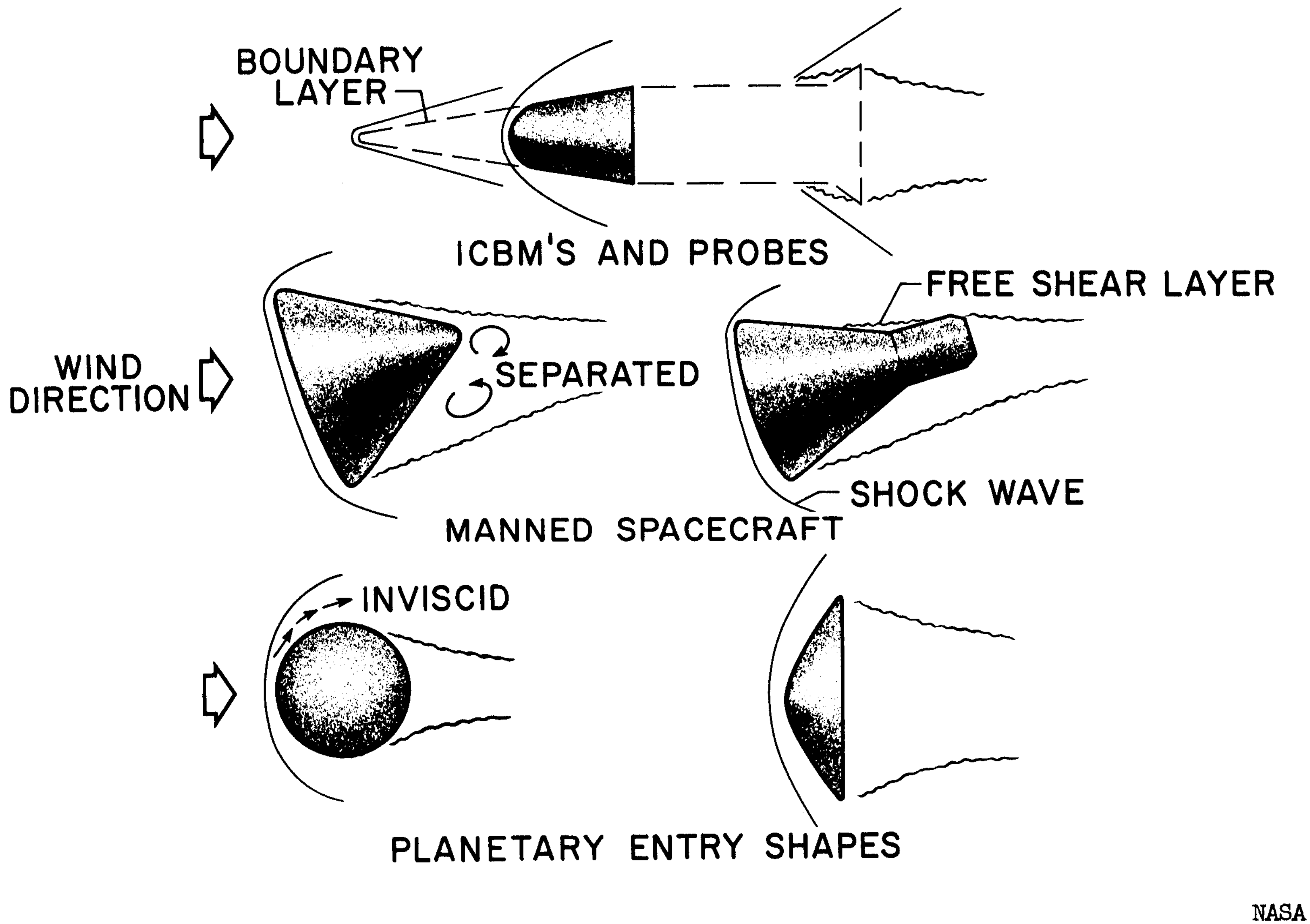

Figure 1.- Reentry flow-field plasmas.

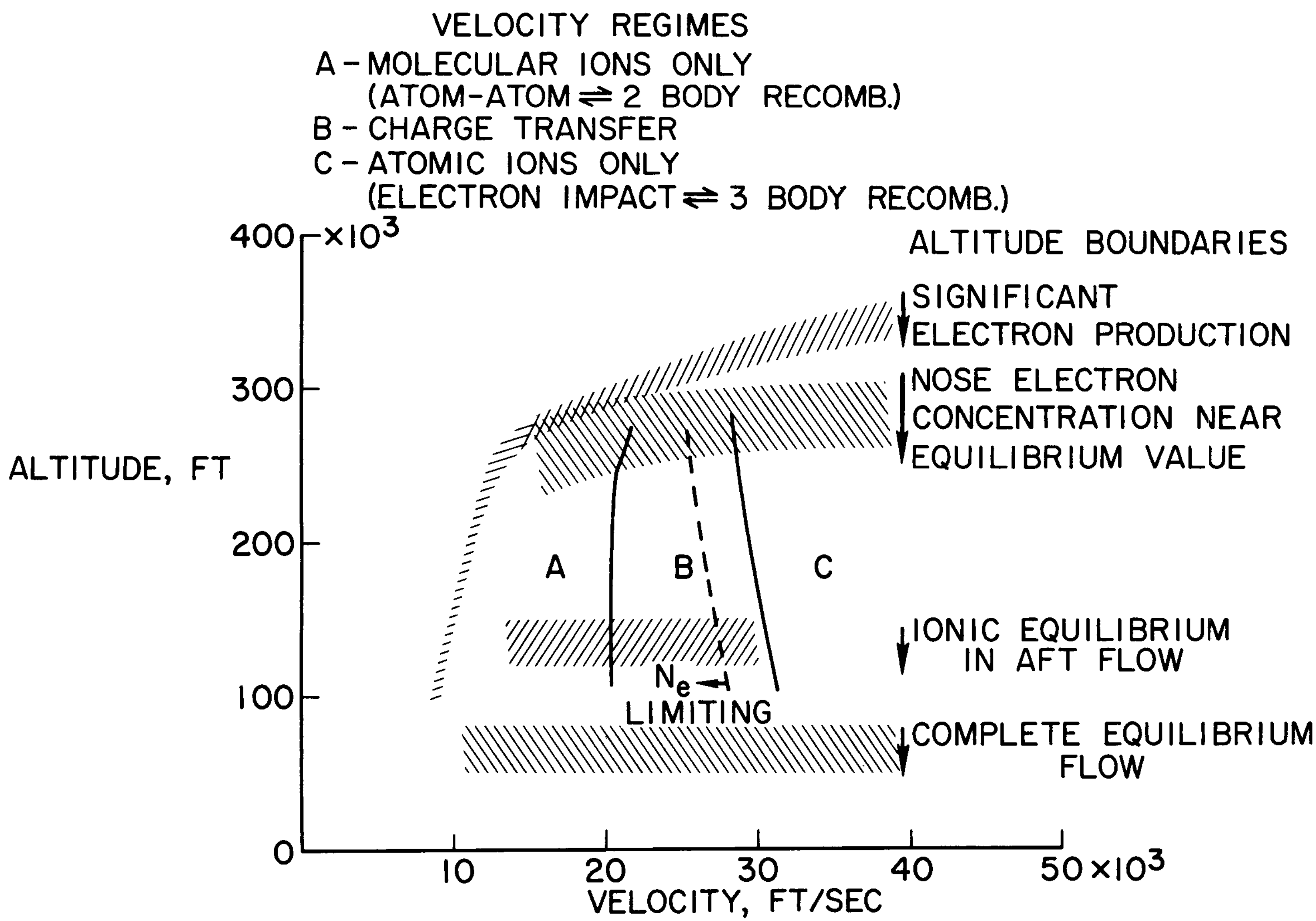

NASA

Figure 2.- Ionic chemical-kinetic regimes for blunt-body reentry.

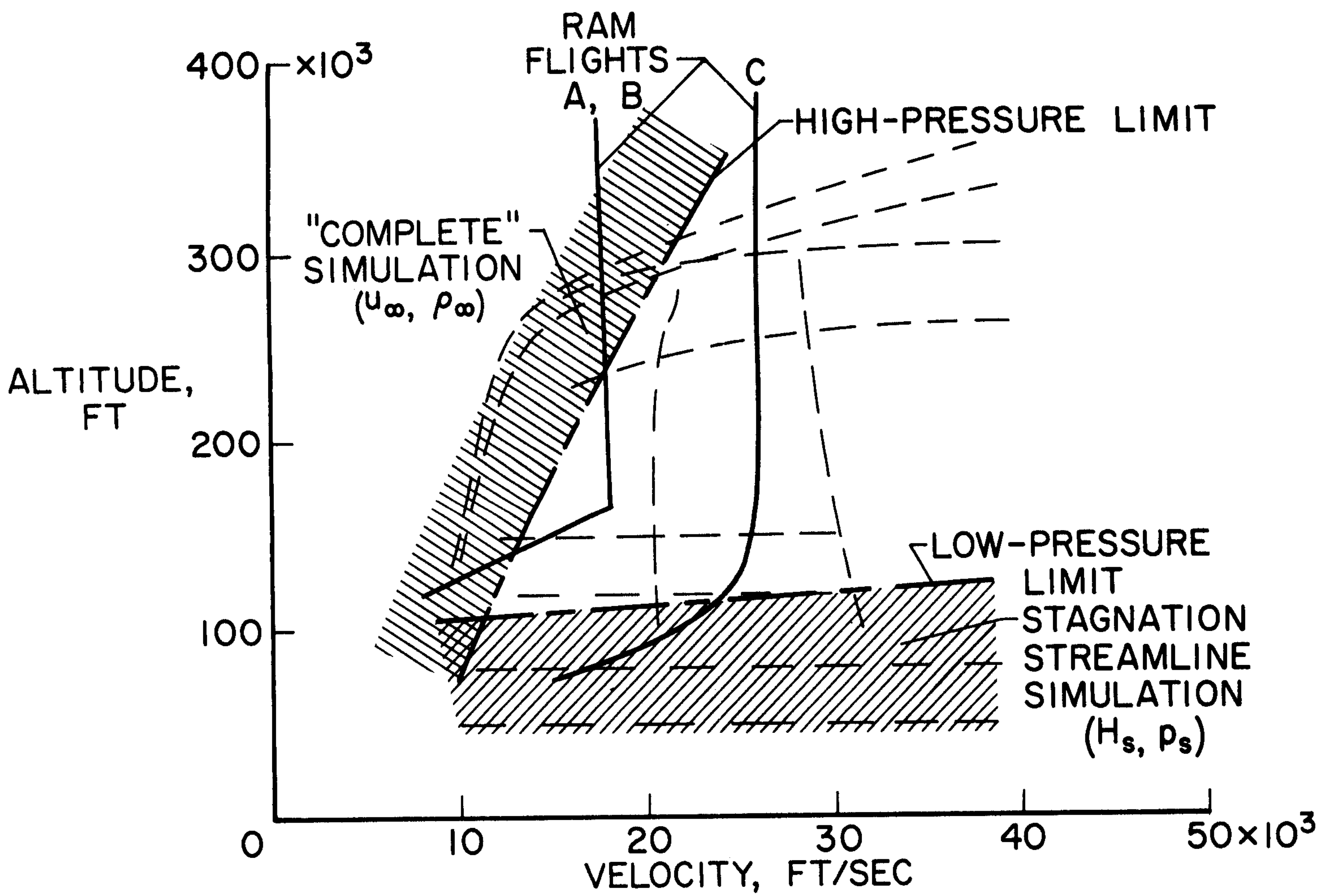

NASA

Figure 3.- Shock-tunnel flow-field simulation.

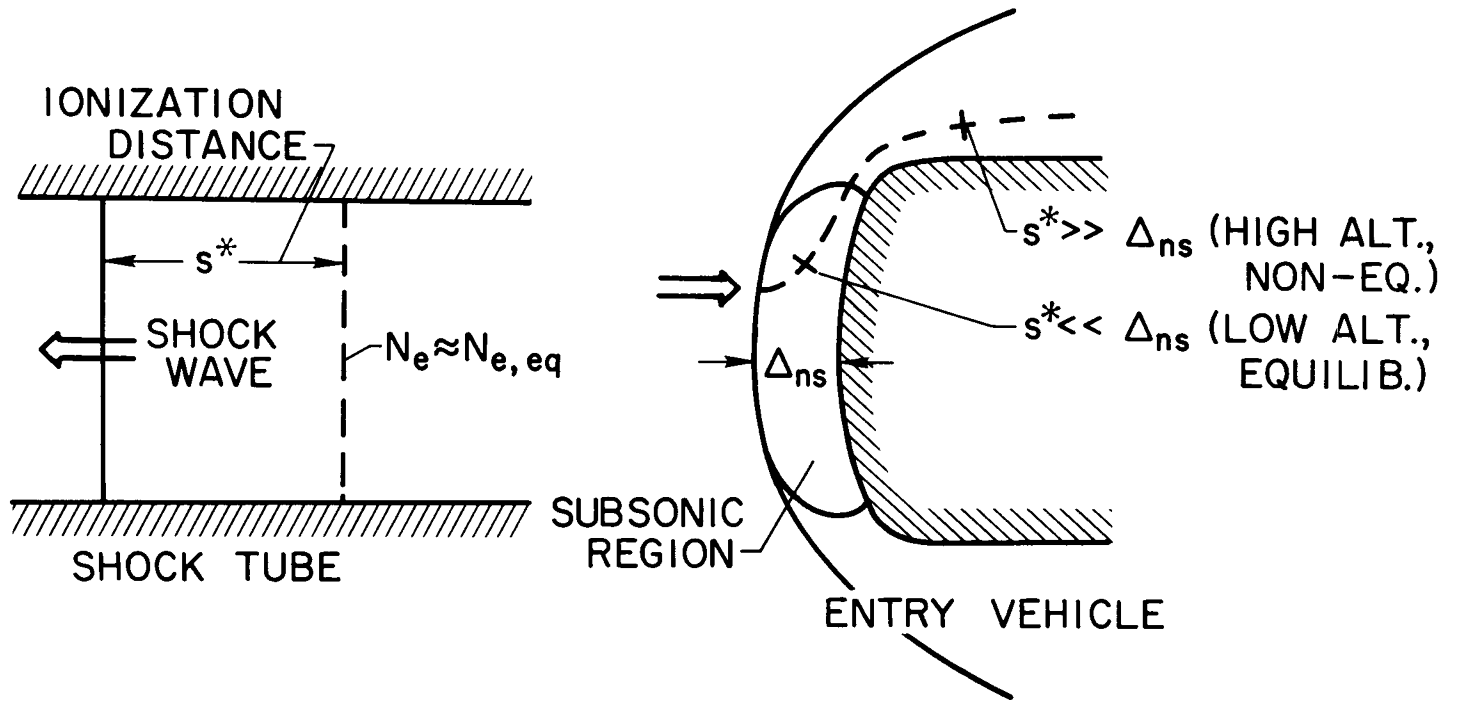

NASA

Figure 4.- Nose-flow nonequilibrium ionization.

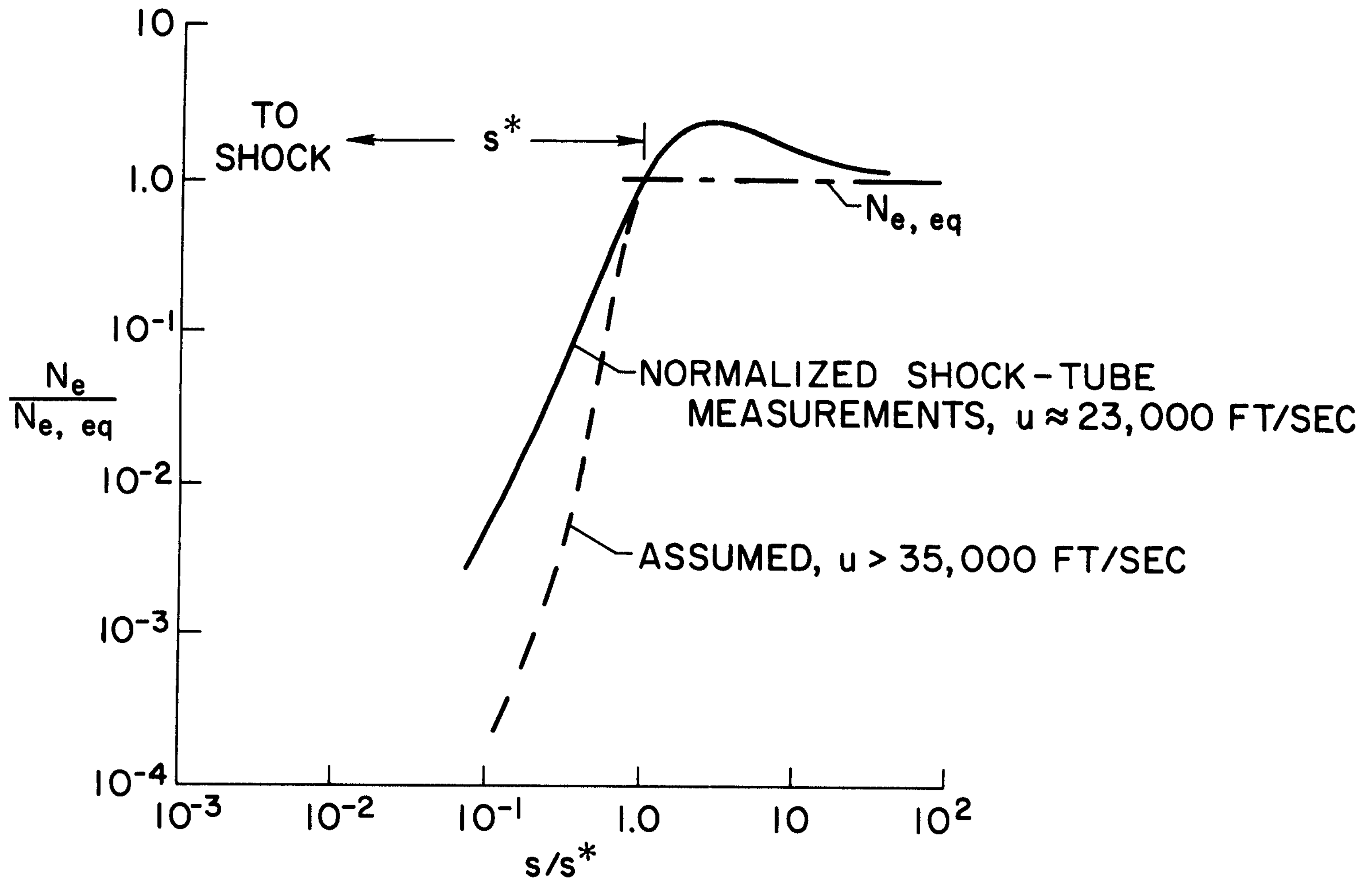

NASA

Figure 5.- Shock-wave ionization.

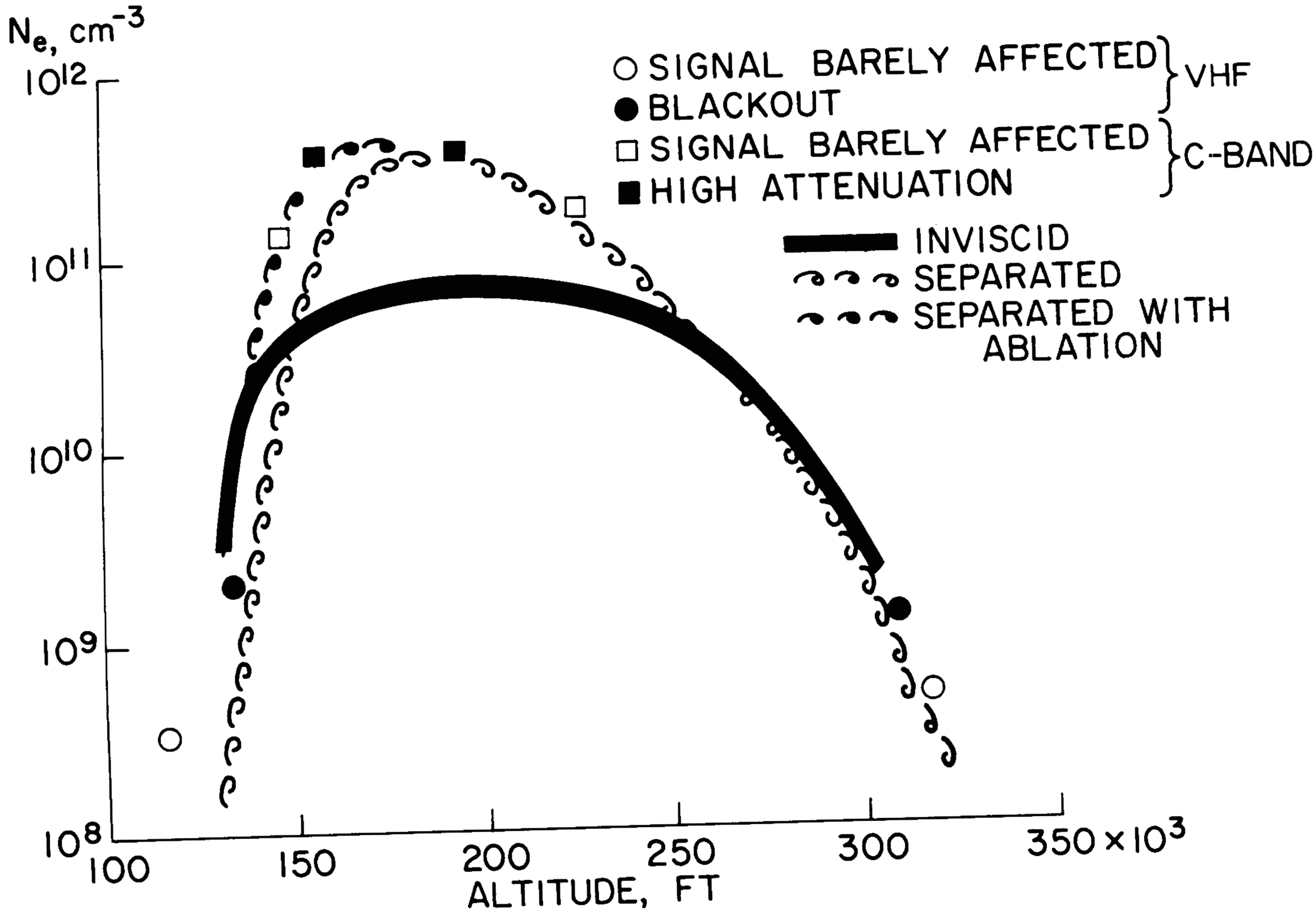

NASA

Figure 6.- Flow-field electron densities for Mercury-Atlas flights.

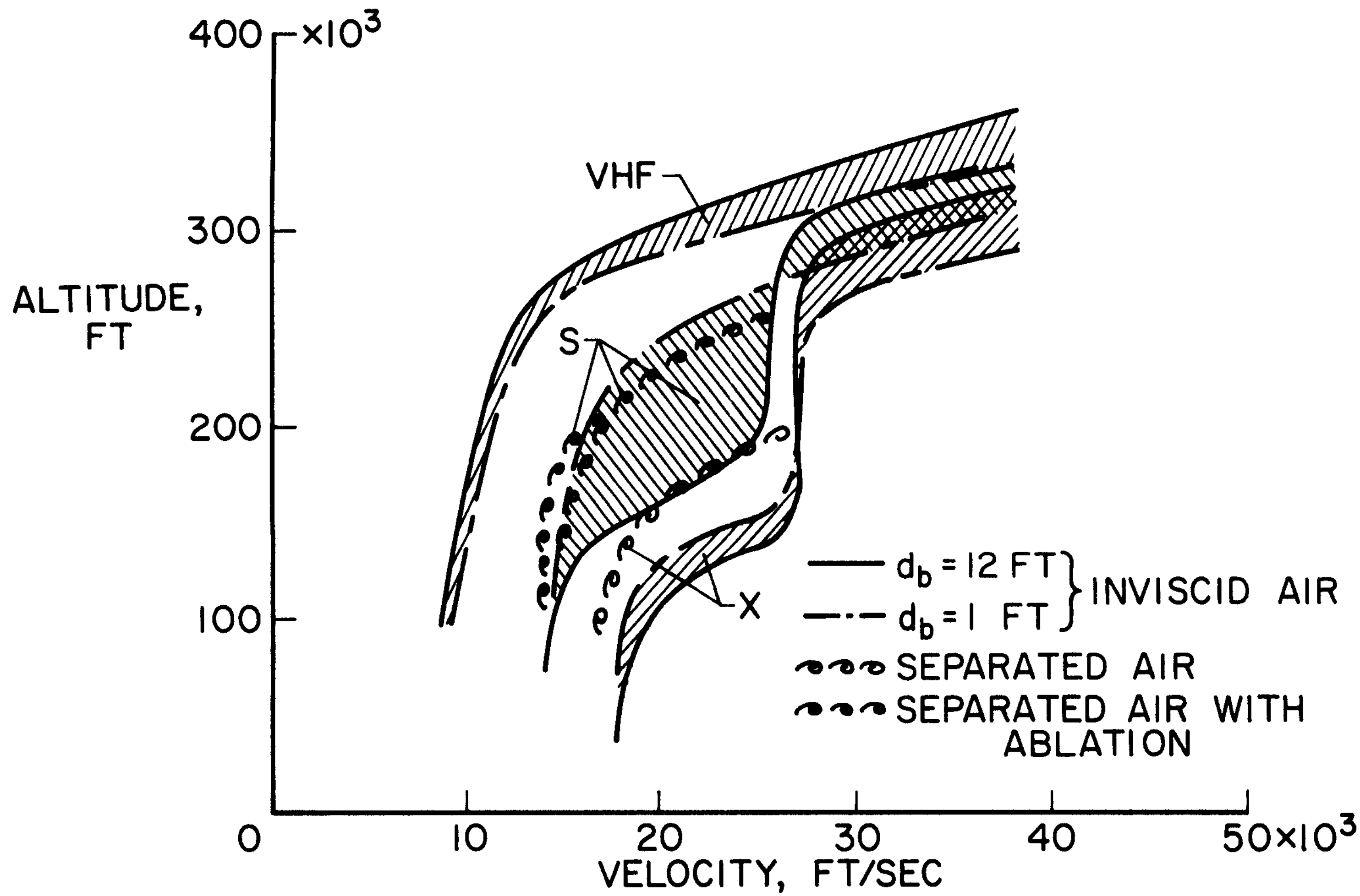

NASA

Figure 7.- Estimated signal blackout bounds for blunt bodies.

NASA-Langley, 1965